ICW note 1854

february 1988

nota

instituut voor cultuurtechniek en waterhuishouding, wageningen

DIURNAL VARIATION OF BARE SOIL REFLECTANCE

ing. W.G.M. Bastiaanssen

C O N T E N T S

1. INTRODUCTION

The reflected radiant energy of a natural body is dependant on the surface characteristics of the body and the wavelength of the incident radiant energy. Information on the surface can be obtained if the reflectance at a fixed wavelength interval, e.g. the total solar spectrum, is known. The problem addressed here, is that surface reflectance shows a diurnal variation which can be even different from day to day. It is of common interest to describe this diurnal reflectance behaviour physically. When a theory for the environmental dependant surface reflectance is designed, the surface reflectance can be computed for each condition of the atmosphere. In order to classify surfaces on basis of reflectance, a reference surface reflectance have to be defined. Because incident irradiance and reflected irradiance effects the net radiation considerably, energy processes at the surface can be assessed with more accuracy in respect to time.
The figures in the present report are based on measurements of surface reflectance in arid regions. The new derived reflectance equation is partly applicable in humid climates, because observations were performed under cloudy conditions as well. The surface reflectance plays a key role in the framework of a remote sensing project, towards the actual evaporation in deserts (title: "mapping evaporation from playas in North Africa"). Fieldwork has been carried out in the Western desert of Egypt, where large natural depressions in combination with a shallow watertable are found (playa, Arab: sebkha). A large level of salinity keeps the surface mostly free from natural vegetation.

2. REFLECTED RADIANT ENERGY

2.1. Importance of surface reflectance

Natural materials will reflect, absorb, scatter and transmit shortwave solar irradiance. According MONTEITH (1973), different definitions of reflected energy have to be distinghuised; the surface reflectivity is the fraction of incident solar irradiance reflected at specific wavelength while the reflection coefficient or albedo is the reflectivity integrated over the total solar spectrum. The term reflectance shall be applied in the present report, which is equal to the reflection coefficient.

The reflectance of a particular surface can be obtained by dividing the reflected irradiance by the incident irradiance (0.3 μm-2.8 μm). The reflectance is dependent on the characteristics of that surface. This implicates an important tool for many investigations:

- discrimination of different surface types; airborne and spaceborne classifications of all kinds of surfaces can be made when the absorption behaviour of the surfaces involved are known;
- conditions of specific surface type; when more about the surface is known e.g. soil type and the water content, estimations of the particle diameter of minerals can be obtained;
- areal pattern of available net radiation; the shortwave radiation budget appears to be the major component of net radiation. Thermal radiometers present in todays satellite series, can be used for the determination of the net longwave radiation.
  Combination results in values of net radiation;
- quantitative analyses of energy processes through Earth's surface;
  This are the latent heat, soil heat and sensible heat fluxes.
  a) energy fluxes can be computed from groundbased observations, applying commonly accepted radiation equations;
  b) energy fluxes can be computed from space and airborne observations, applying linear functions describing the relationship between those fluxes and the surface reflectance and surface radiation temperature (MENENTI, 1984).

The surface reflectance appears however not to be a constant for a particular type of soil. It varies with the following items:
- view angle (sun zenith angle, micro relief);
- ratio diffuse to total irradiance (cloudiness, dust);
- soil water content of the surface toplayer;
- soil bulk properties (organic matter, particle size, mineralogy);
- vegetation cover;
- salt solutes of the surface toplayer;
- surface roughness (cultivation, erosion).

For diurnal considerations, the former 3 properties cannot be considered as being constant. An attempt will be made to relate the solar elevation, the diffuse component of the total irradiance and the drying wetting cycle mathematically with the actual surface reflectance. A proper description of the diurnal variation gives a better estimation of the mean daily surface reflectance. With respect to the moment of satellite overflight (e.g. Landsat: early morning), a better time dependant reflected radiant energy budget can be estimated. Net radiation values and consequently all surface energy fluxes can be determined in timesteps much smaller than on daily basis. It opens also possibilities to establish reflectances at reference weather conditions so that mutually comparison between surfaces can be made (classification). Bidirectional surface reflectance can be assessed when the topography in relation to a horizontal plane and solar elevation is known.
Remote sensing recordings are only succesfull when cloudless skies are present. So, remotely sensed reflectance data is only available on sunny days where the surface is an imperfect diffuse reflector with consequently large oscillations of the surface reflectance.

2.2. Expressions on reflection variation

The diurnal variation of surface reflectance has been described by many authors (MAKAROVA (1973), ROSS (1975), LARSON and BARKSTROM (1977), BARTMAN (1980)). Limitation of all these equations is the difficulty of deriving the regression coefficients or the incomplete

dependancy on the diurnal change of physical processes. Bartman designed a relationship between surface reflectance (α_0) and sun zenith angle (ϕ_{su}) according:

$$\alpha_0 = \alpha_0' \; 2.444 \; [1 - \cos\phi_{su} \; \ln \; (1 + \frac{1}{\cos\phi_{su}})] \qquad (1)$$

where α_0' is the surface reflectance at $\phi_{su} = 0$. Some critical remarks regarding these equation are the absence of atmospherical influences and the confusion around α_0'. Namely at $\phi_{su} = 0$, the equation still reads $\alpha_0 = \alpha_0' \; 0.75$ which is not in fully agreement with the defenition of α_0'. The neglected influence of diffuse radiation will result in bad fitting between the measured and calculated surface reflectance curves.

Moist soil surfaces react with more absorption of the shortwave irradiance than dry soil surfaces do. The relation with soil water content (θ) can be satisfactorilly described (MENENTI, 1984) with the following set of equations:

$$\alpha_0 = \alpha_{0dry} \; (\frac{x - \theta}{x}) + \alpha_{water} \; \frac{\theta}{x} \qquad \text{if} \quad \theta \leqslant \theta^* \qquad (2)$$

$$\alpha_0 = \alpha_{0sat} \qquad \text{if} \quad \theta^* < \theta < x \qquad (3)$$

$$\alpha_{0sat} = \frac{\alpha_{0dry}}{[n^2 \; (1 - \alpha_{0dry}) + \alpha_{0dry}]} \qquad (4)$$

where x (-) is the total soil porosity, θ ($cm^3.cm^{-3}$) the water content at surface level, θ^* ($cm^3.cm^{-3}$) a treshold of water content where the water film breaks down and n (-) the refraction index of the saturating liquid. PLANT (1970) showed that n is usefull to relate with salt solutes. The linear dependancy described in eq. (2) was confirmed by VAN DEN BERGH and BOUMAN (1986), who found also a linear relation between absorption and water content:

$$k = k_{dry} + \theta\, k_{water} \qquad (5)$$

where k (-) is the coefficient of absorption of the total soil mass, k_{dry} (-) the coefficient of absorption of the dry soil mass, k_{water}(-) the coefficient of absorption of the soil water and θ ($cm^3.cm^{-3}$) the volumetric soil water content. Disadvantage of eq. (2) is that on site α'_{0dry} and θ values of the drying surface are hardly available because continuous measurements of hypersaline soil water content requires quite advanced techniques and surface reflectance values of completely dry soils can only be achieved at laboratories. Further, the water content where the film breaks down (θ^*) is difficult to determine under field conditions. Hence the combination of (2) with other reflectance equations like eq. (1), (6) and (7) is only applied if θ values throughout the morning and α'_{0dry} figures are available.
MAKAROVA (1973) proposed an expression which accounts both on the view angle and the diffuse component of the irradiance:

$$\alpha_0 = \alpha'_0 \left[1 + 2.5 \left(1.25 - \frac{R_{swdf}}{R_{sw}}\right) (1 - \alpha'_0) \sin 1.5\, \phi_{su}\right] \qquad (6)$$

where R_{swdf} ($w.m^{-2}$) is the diffuse irradiance and R_{sw} ($w.m^{-2}$) the incident irradiance. This implicit equation is difficult to solve analytically and not handy to derive eventually new regression coefficients from field observations. One have to be noted that large diffuse irradiance patterns results in low reflectance values.
ROSS (1975) suggested a relationship between view angle (ϕ_{su}) and surface roughness (b):

$$\alpha_0 = \frac{\alpha'_0}{1 + b \sin (1 - (90 - \phi_{su}))} \qquad (7)$$

Good agreements between $\alpha_0 = \alpha_0(\alpha'_0, b, \phi_{su})$ where found for grassland, applying the TERGRA model (SOER et al., 1980). Absence of atmospherical conditions makes these handy equation alas incomplete.

2.3. Features of reflectance in arid regions

Measurements in the Western desert of Egypt indicated significant diurnal variations of surface reflectance. The larger the ratio R_{swdf}/R_{sw}, the lower the fluctuations of reflectance appear to be a rule of thumb. The reflectance increases rapidly after 4 p.m., which is a result of simultaneous decreasing of the solar altitude and increasing of the ratio diffuse to total irradiance. Sunset was recorded at 17.40' while the sun rises up at 6.40' (local time). Different phenomena can be noticed during the morning; when the morning reflectance is much lower than the noon reflectance (see Fig. 1A), dew will be present in large quantaties. If the morning reflectance appears to be larger than the noon reflectance, the temporary surface wetting was not present (see Fig. 1B).

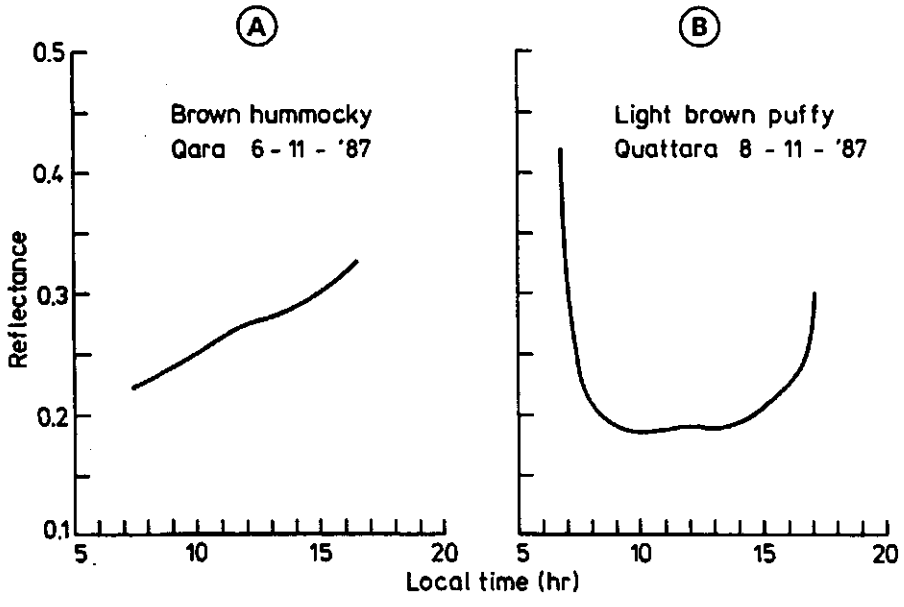

Fig. 1. Measured surface reflectances, Qara oasis, November 1987

3. DATA COLLECTION SCHEME

Three fieldcampaignes were performed towards the natural depressions in the Western desert of Egypt. The first campaign has taken place from 25 July through 10 August 1986, the second campaign from 8 February through 28 March 1987 and the third campaign from 16 Oktober through 27 November 1987. Mainly non-vegetated hypersaline playas with a shallow groundwater table were selected. To complete the insight of reflectance behaviour, experiments from the Lybian Desert as obtained by MENENTI (1978) are added to the analyses.

Table 1. Overview data collection scheme Egyptian and Lybian deserts

Period	Site	Longitude	Latitude	Number of surfaces
6 - 28 Feb. 1978	W Idri	10°20'	27°40'	1
12 - 17 Feb. 1978	NE Idri	10°20'	27°40'	1
17 - 20 Feb. 1978	NNW Idri	10°20'	27°40'	1
20 - 24 Feb. 1978	Idri	10°20'	27°40'	1
27Aug-21 Sept 1978	W Idri	10°20'	27°40'	1
30Aug-4 Sept 1978	NE Idri	10°20'	27°40'	1
5 - 8 Sept 1978	Idri	10°20'	27°40'	1
1 - 3 Aug. 1986	Bir Sharib	28°30'	30°15'	1
4 - 5 Aug. 1986	Moghra oasis	28°35'	30°18'	1
26 - 27 Feb. 1987	Bir Tarfawi	28°52'	22°58'	5
6 March 1987	Bir Sharib	28°30'	30°15'	4
9 - 10 March 1987	SE Siwa	25°38'	29°09'	5
11 - 13 March 1987	W Siwa	25°29'	29°13'	5
14 - 16 March 1987	E Siwa	25°38'	29°16'	5
4 - 6 Nov. 1987	NE Qara	26°33'	29°37'	4
8 - 9 Nov. 1987	Quattara depr.	26°45'	29°24'	4
11 - 13 Nov. 1987	Qaneitra muhasas	26°53'	29°44'	4

Recordings were done with a set of pyranometers of which the downwards looking pyranometers registrate the reflected irradiance and the upwards looking pyranometers the incident irradiance. Additional diffuse irradiance measurements were done by means of a pyranometer with a shadow ring during the 3rd field campaign. The observations were registrated automatically via a datalogger to a personal computer.

4. REGRESSION METHODOLOGY

4.1. Concept

A new regression equation has to be specified, matching the comments given in chapter 2. The problem is to find a rather simple regression equation which deals with all phenomena. A solution has been found by a non-linear regression function off the following type:

$$Y = a \cdot c^{X} \qquad (8)$$

If X is substituted by sin ϕ_{su} and Y by α_0, the regression coefficient a becomes α_0 at $\phi_{su} = 0$. Thus coefficient a can be defined as α_0' i.e. α_0 ($\phi_{su} = 0$). The directional reflectance equation can then be read as:

$$\alpha_0 = \alpha_0' \, c^{\sin\phi_{su}} \qquad (9)$$

The improvements are:

- regression coefficients α_0' and c can both statistically related with measured field reflectances and observed zenith angles, applying a simple non-linear regression equation: Ln α_0 = Ln α_0' + sin ϕ_{su} Ln c (see Fig. 2);
- the shape of the reflectance versus time curve is not longer fixed i.e. the regression coefficient c is an empirical variable which have to be related with atmospherical conditions;
- the equality $\alpha_0 = \alpha_0'$ at $\phi_{su} = 0$ remains valid.

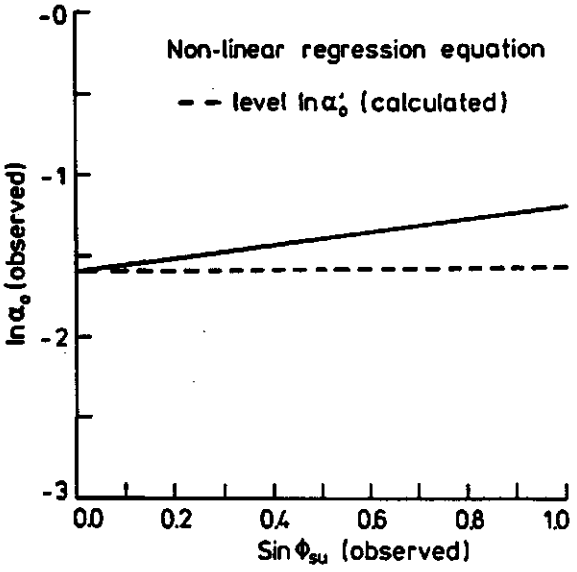

Fig. 2. A new non-linear regression equation

Observed reflectance and sun zenith figures were applied to derive the best fitting combination of α_0' and c (see table 2). Because of diurnal considerations, the time scale was chosen on daily basis. The c values for a particular day were found to be in the same order of magnitude! This confirms that the $\bar{c}$ regression coefficient, i.e. the mean daily c coefficient, is indeed related with the mean daily weather conditions. Such an analyses can only be established in terms of data collection covering whole the day, at least from 8 a.m. until 4 p.m.. Seperated days with different degrees of mean cloudiness have to be considered.

Table 2. Calculated regression coefficients, 3rd fieldcampaign

Date	Site	Surface	α_0'	$\bar{c}$	mean $\bar{c}$	stand. dev.	time
5/11	Qara oasis	Sandcrust on ped.	0.181	2.724	2.811	0.390	8.05-17.20
5/11	Qara oasis	Grey puffy	0.182	2.436	2.811	0.390	8.05-17.20
5/11	Qara oasis	Brown hummocky	0.124	2.639	2.811	0.390	8.05-17.20
5/11	Qara oasis	White salt crust	0.185	3.446	2.811	0.390	8.05-17.20
6/11	Qara oasis	Sandcrust on ped.	0.310	1.339	1.130	0.123	7.25-16.50
6/11	Qara oasis	Grey puffy	0.366	1.039	1.130	0.123	7.25-16.50
6/11	Qara oasis	Brown hummocky	0.254	1.099	1.130	0.123	7.25-16.50
6/11	Qara oasis	White salt crust	0.479	1.044	1.130	0.123	7.25-16.50
8/11	Quattara	Brown puffy	0.080	3.469	4.049	0.612	6.35-17.20
8/11	Quattara	Brown puffy	0.082	3.661	4.049	0.612	6.35-17.20
8/11	Quattara	Brown puffy	0.054	5.054	4.049	0.612	6.35-17.20
8/11	Quattara	Sandy soft clay	0.068	4.013	4.049	0.612	6.35-17.20
11/11	Qaneitra	Grey brown puffy	0.069	5.472	4.303	1.168	10.35-17.15
11/11	Qaneitra	Grey brown puffy	0.109	3.13	4.303	1.168	10.35-17.15
12/11	Qaneitra	Grey brown puffy	0.103	3.080	2.863	0.511	6.25-17.15
12/11	Qaneitra	Sandcrust	0.205	2.033	2.863	0.511	7.20-17.15
12/11	Qaneitra	Grey brown puffy	0.119	2.646	2.863	0.511	6.25-17.15

4.2. Atmospherical conditions

Experimental $\bar{c}$ values have to be related with the atmospherical conditions on that particular day. Clouds have the most direct effect on radiant transmittance (CARLSON and WENDLING, 1977). Presence of clouds and dust will result in more scattering effects, more incident reflectance by clouds and a higher absorption by atmospheric gases and aerosols. The radiation distribution will only tend to be a perfect Lambertian surface when diffuse irradiance is abundantly present.
The atmosperical transmittance can be expressed in terms of the optical depth or the ratio diffuse (R_{swdf}) to total irradiance (R_{sw}).

4.2.1. Optical depth of Earth's atmosphere

The mean daily optical depth can be given by:

$$\tau = - \ln \left(\frac{\overline{R_{sw}}}{\overline{R_{sw\text{-}out}}} \right) \qquad (10)$$

where τ (-) is the mean daily optical depth, $\overline{R_{sw}}$ ($w.m^{-2}$) the mean daily irradiance and $\overline{R_{sw\text{-}out}}$ ($w.m^{-2}$) the mean daily solar energy at the top of the atmosphere. The latter parameter can be easily read from Milankovitch tables (see Smithsonian Meteorological table 132). The extra-terrestrial radiance is given on daily basis sothat the time unit of the optical depth cannot be smaller. Disadvantage of such tables is that the radiation values are given as a latitude dependant mean variable.
Special attention have to be paid to obtain reliable $\overline{R_{sw}}$ values. A complete set of reguraly irradiace recordings between sunrise and sunset is seldom available. Therefore a solution was found by taking the absolute integral between sunrise and sunset of next least square function:

$$\int_{\text{sunrise}}^{\text{sunset}} a + bt + ct^2 \, dt \qquad (11)$$

Table 3. Regression coefficients of the daily incident irradiance function as obtained by the least square method, 3rd fieldcampaign

Date	Site	a	b	c
5/11	Qara oasis	0.85	115.73	- 6.15
6/11	Qara oasis	0.24	68.89	- 2.68
8/11	Quattara depression	0.64	193.80	-11.09
11/11	Qaneitra muhasas	0.54	191.26	-10.95
12/11	Qaneitra muhasas	0.29	68.89	- 2.77

4.2.2. Ratio of diffuse to total irradiance

Fluctuations of the ratio R_{swdf}/R_{sw} was often noticed. It can be stated that the ratio R_{swdf}/R_{sw} increase by decreasing of the solar altitude (see Fig.3). To obtain $\overline{R_{swdf}}$ values, the similar procedure as deriving $\overline{R_{sw}}$ values can be followed (see table 4).

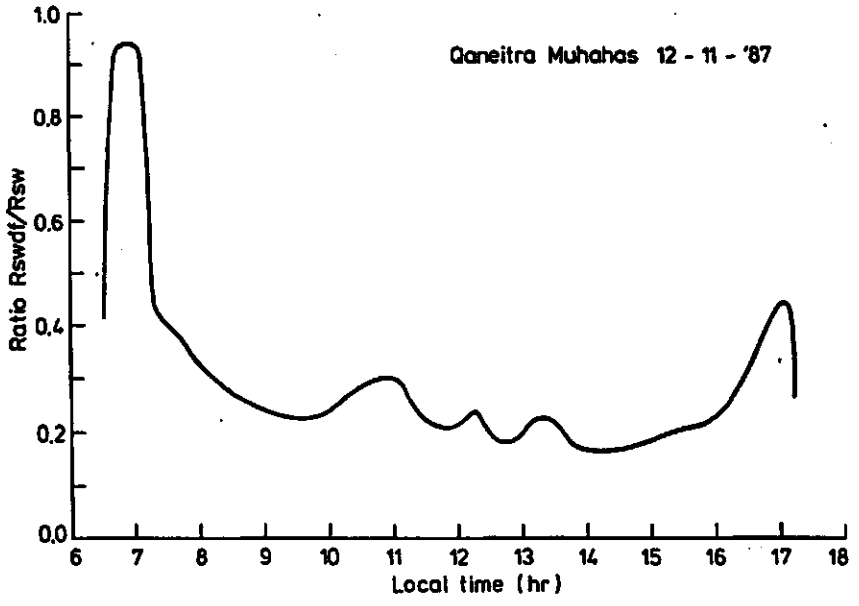

Fig. 3. Support of diffuse radiation on the shortwave radiation budget

Table 4. Regression coefficient of the daily diffuse irradiance function as obtained by the last square method, 3rd fieldcampaign

Date	Site	a	b	c
5/11	Qara oasis	0.24	37.72	-1.74
6/11	Qara oasis	0.20	43.85	-2.21
8/11	Quattara depression	0.04	16.02	-0.76
11/11	Qaneitra muhasas	0.05	18.23	-0.92
12/11	Qaneitra muhasas	0.09	19.82	-0.88

4.2.3. Statistical relationships

Up till now the dependancy of $\bar{c}$ upon $\overline{R_{swdf}}/\overline{R_{sw}}$ and $\overline{R_{sw}}/\overline{R_{sw-out}}$ was discussed but not algebraically related. This can be done after comparison between both alternatives. Because of the availability of $\overline{R_{swdf}}/\overline{R_{sw}}$ measurements, the comparison could only be made for figures gathered during the third fieldcampaign (see table 5).

Table 5. Overview mean daily atmospherical conditions, 3rd fieldcampaign

Date	$\bar{c}$ (-)	$\overline{R_{swdf}}$ ($w.m^{-2}$)	$\overline{R_{sw}}$ ($w.m^{-2}$)	$\overline{R_{sw-out}}$ ($w.m^{-2}$)	$\overline{R_{swdf}}/\overline{R_{sw}}$ (-)	$\overline{R_{sw}}/\overline{R_{sw-out}}$ (-)	τ (-)
5/11	2.811	53	187	285	0.283	0.656	0.42
6/11	1.130	79	181	282	0.438	0.642	0.44
8/11	4.049	32	256	278	0.125	0.921	0.08
11/11	4.303	33	252	273	0.131	0.923	0.08
12/11	2.863	44	175	272	0.251	0.643	0.44

The correlation coefficient (r) between $\bar{c}$ and $\overline{R_{swdf}}/\overline{R_{sw}}$ is 0.99 (see Fig. 4) and is strictly speaking quite favourable than r = 0.84 between $\bar{c}$ and τ. The less favourite fitting with τ is however still in agreement with the supposed theory. Especially when no $\overline{R_{swdf}}/\overline{R_{sw}}$ data is available (which is often the case), τ values may be very helpfull. This can be done since irradiance is mostly sensed at any officially meteorological station. Hence, the best linear regression fit can be made with the ratio $\overline{R_{swdf}}/\overline{R_{sw}}$.

$$\bar{c} = 5.42 - 9.71 \frac{\overline{R_{swdf}}}{\overline{R_{sw}}} \qquad (12)$$

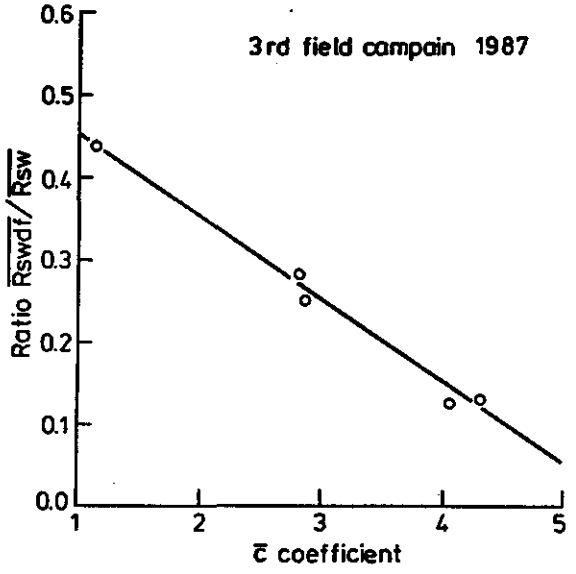

Fig. 4. Linear equation relating the ratio $\overline{R_{swdf}}/\overline{R_{sw}}$ with the $\bar{c}$ regression coefficient

Eq. (12) has a permitted range of $\overline{R_{swdf}}/\overline{R_{sw}}$ between 0.12 - 0.44. Outside this range, such as in humid climates, new datapoints of $\bar{c}$ and $\overline{R_{swdf}}/\overline{R_{sw}}$ have to be determined. It must be again emphasized that the ratio $\overline{R_{swdf}}/\overline{R_{sw}}$ is based on daily basis. At smaller time steps e.g. 30 minutes, the equation becomes approxiametly:

$$c = \bar{c} - (\bar{c} - 1) \frac{R_{swdf}}{R_{sw}} \qquad (13)$$

By this way, the lower limit of the c coefficient is fixed at one. Combination of the analyses of 2nd and 3rd fieldcampaign lead to table 6. The data of the 1st fieldcampaign in 1986 appeared to be incomplete and not applicable for this type of analyses.

Table 6. Optical depths and $\bar{c}$ regression coefficients for 2nd and 3rd fieldcampaign

Date	Site	τ	$\bar{c}$
26/2	Bir Tarfawi	0.18	1.895
12/3	Siwa oasis	0.05	1.922
15/3	Siwa oasis	0.60	1.689
5/11	Qara oasis	0.42	2.811
6/11	Qara oasis	0.44	1.130
8/11	Quattara depression	0.08	4.049
11/11	Qaneitra muhasas	0.08	4.303
12/11	Qaneitra muhasas	0.44	2.863

The following regression function describes correctly the $\bar{c}=\bar{c}(\tau)$ relationship ($r = 0.84$):

$$\bar{c} = 3.36 - 2.71\ \tau \qquad (14)$$

4.2.4. Lybian verification

It is of outstanding interest to compare the derived $\bar{c}(\tau)$ relationship of Egypt with the fieldwork gathered in the Lybian desert, 1978. This additional information may improve the reliability of eq. (14). Different types of playa crusts at different periods have been selected. The reflected irradiance was measured on 2 different spots simultaneously.

Table 7. Investigation on reflectance in the Lybian Desert, 1978

Date	Site	Surface	$\overline{R_{sw}}$ ($w.m^{-2}$)	$\overline{R_{sw-out}}$ ($w.m^{-2}$)	$\bar{c}$ (-)	mean $\bar{c}$ (-)	τ (-)
9/2	Playa West Idri	Wet sebkha	208	302	2.569	2.569	0.373
11/2	Playa West Idri	Wet sebkha	208	306	1.657	2.479	0.386
11/2	Playa NNW Idri	Water sebkha	208	306	3.300	2.479	0.386
14/2	Playa West Idri	Wet sebkha	248	313	1.413	1.316	0.371
14/2	Playa NE Idri	Dry sebkha	248	313	1.219	1.316	0.371
15/2	Playa West Idri	Wet sebkha	216	315	2.530	2.095	0.239
15/2	Playa NE Idri	Dry sebkha	216	315	1.660	2.095	0.239
21/2	Playa West Idri	Wet sebkha	258	328	3.397	3.463	0.240
21/2	Idri	Irrigated palms	258	328	3.528	3.463	0.240
22/2	Playa West Idri	Wet sebkha	243	330	3.206	3.824	0.306
22/2	Idri	Irrigated palms	243	330	4.442	3.824	0.306
2/9	Playa West Idri	Extremely dry	318	417	1.331	1.427	0.271
2/9	Playa NE Idri	Dry sebkha	318	417	1.523	1.427	0.271
4/9	Playa West Idri	Extremely dry	317	413	1.144	1.250	0.265
4/9	Playa NE Idri	Dry sebkha	317	413	1.356	1.250	0.265
6/9	Playa West Idri	Extremely dry	320	410	1.222	1.638	0.248
6/9	Idri	Palms on dunes	320	410	2.054	1.638	0.248
8/9	Playa West Idri	Extremely dry	297	406	1.160	1.641	0.313
8/9	Idri	Palms on dunes	297	406	2.121	1.641	0.313

Totally 10 new regression points became available. They were put together with the 8 regression points from Egypt, which finally can be fitted with:

$$\bar{c} = 3.12 - 2.58\ \tau \qquad (15)$$

However the regression coefficient of eq. (15) is lower than eq. (14), with r = 0.72 and r = 0.84 respectively, eq. (15) will be considered on basis of the larger number of datapoints. Hence eq. (14) will be replaced by eq. (15).

4.3. Wetting drying cycle

Low air temperatures during the early morning (5 a.m.) and atmospherical contact with hypersaline playa soils, will cause a high relative humidity with consequently spores of condensation on the soil surface. The thin dew film (app. 0.4 mm) absorpts radiant energy effecting the surface reflectance. The evaporation of dew will take about 5 hours to disappear again (MENENTI et al.,1986). The procedure is to relate dew with the actual reflectance according a linear relationship as presented in paragraph 2.2. Here the term α_{0dew} is introduced, which parameter can be conceived as a dummy reflectance factor just after sunrise. Values of α_{0dew} can be calculated from measured α_0 and calculated $\bar{c}$ figures by inversion of eq. (9):

$$\alpha_{0dew} = \frac{\alpha_0}{\bar{c} \sin \phi_{su}} \qquad (16)$$

In fact, the ratio α_{0dew}/α'_0 is another expression for the soil water content of the surface. This new idea has been checked against calculated values of α_{0dew} (eq. (16)) and field observations of θ, where soil water samples were collected at 7 a.m. and 5 p.m. (see table 8).

Table 8. Surface reflectance in relation with soil water content 3rd fieldcampaign

Date	Surface	α_{0dew}/α'_0 (-)	$d\theta$ ($cm^3.cm^{-3}$)	$d\alpha_0$ (-)	$d\alpha_0/d\theta$ ($cm^3.cm^{-3}$)
6/11	Brown hummocky	0.93	0.01912	0.027	1.41
9/11	Brown puffy	0.83	0.06754	0.014	0.21
9/11	Brown puffy	0.83	0.05423	0.014	0.26
9/11	Sandy soft clay	0.75	0.10515	0.017	0.16
12/11	Grey brown puffy	0.81	0.06028	0.020	0.33
12/11	Sandcrust	0.85	0.05940	0.032	0.54
12/11	Grey brown puffy	0.80	0.09768	0.024	0.25

The trend shown between α_{0dew}/α_0' and θ is quite logical ($r = 0.71$). This allows for more investigation of the ratio α_{0dew}/α_0' which can be conceived as a dummy dew factor (see table 9); a low ratio of α_{0dew}/α_0' indicates clear spores of condensation while at the other hand a ratio of 1.0 shows no effect of the temporary water film at all. The average ratio α_{0dew}/α_0' is 0.81.

Table 9. Dew sensitivity estimations for different types of surface
3rd fieldcampaign

Surface type	α_{0dew}/α_0'	number of replications
Sandcrust on pediment	0.85	2
Puffy	0.78	8
Brown hummocky	0.78	2
White salt crust	1.00	2
Sandy soft clay	0.75	1
Sandcrust	0.75	2

Remarkable is the constant water content of the white salt crust all during the day. The groundwater table was in this situation 15 cm minus groundlevel, which remain the salt minerals very wet. The ratio α_{0dew}/α_0' will gradually change from sunrise upwards until the unity is reached around noon. As mentioned before, this takes about 5 hours sothat α_{0dew}/α_0' becomes constant around 11 a.m.. The time related evaporation rate of dew can be assessed by plotting α_{0dew} versus time, assuming that α_{0dew} and θ are linear related. The grey brown puffy crust on 12 november with $\alpha_0' = 0.119$ and $\bar{c} = 2.646$ has been selected as an example spot.

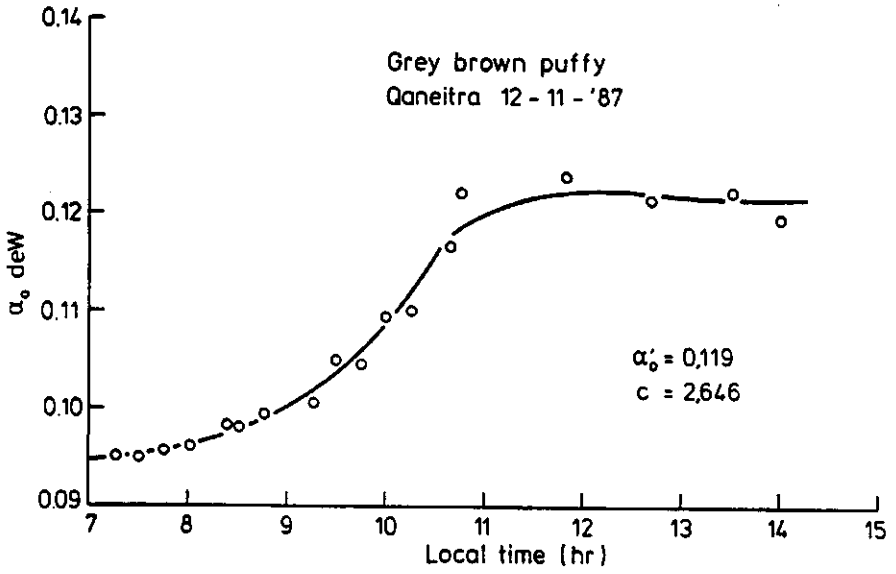

Fig. 5. Time related evaporation of dew

It appears unreasonable that the time dependant evaporation rate is linear. The surface reflectance during the drying period (sunrise - 11.00 a.m.) is therefore suggested to be non-linear:

$$\alpha_0' = \alpha_0' \left[1 - \left(1 - \frac{\alpha_{0\,dew}}{\alpha_0'}\right) \left(\frac{\sin\phi_{su} - \sin\phi_{su^*}}{1 - \sin\phi_{su^*}}\right)\right] \qquad (17)$$

where ϕsu^* is the zenith angle where the temporary water film is changed fully into the gas phase again. Taking $\phi su^* = 49$ at 11.00 a.m. and $\alpha_{0dew}/\alpha_0' = 0.81$ (mean figure 3rd field campaign), eq. (17) becomes a simple goniometric function:

$$\alpha_0' = \alpha_0' \left[1 - (0.772 \sin\phi_{su} - 0.582)\right] \qquad (18)$$

Advantage of this method is that no large series of soil surface water content have to be sampled.

4.4. A new reflectance equation

As shown, a new reflectance equation accounting on view angle, atmospherical conditions and surface water content has been derived. The regression coefficients required for the basic equation can be obtained rather simple from field measurements. The relationship between empirical coefficients and on site conditions have been focussed for arid regions (Egyptian and Lybian deserts). The best accuracy can be obtained when hourly values of the ratio R_{swdf}/R_{sw} are available (group 1c). A convenient fitting curve can also be obtained when the mean daily $\overline{R_{swdf}}/\overline{R_{sw}}$ ratio is known (group 1b). Less accurate, but still applicable is group 1a, where the mean daily optical depth can be computed from incident irradiance. The total set of equations can be finally summarized into groups, which have to be passed by in sequence:

1a. $\bar{c} = 3.12 - 2.58\ \tau$

1b. $\bar{c} = 5.42 - 9.71\ \dfrac{\overline{R_{swdf}}}{\overline{R_{sw}}}$

1c. $c = \bar{c} - (\bar{c} - 1)\ \dfrac{R_{swdf}}{R_{sw}}$

2a. $\alpha_0'(c_2) = \mathrm{Exp}\ (\ln \alpha_0'(c_1) + \sin\phi_{su} \ln c_1 - \sin\phi_{su} \ln c_2)$

(c_1 and $\alpha_0'(c_1)$ known, c_2 calculated from group 1)

3a. $m = [1 - (1 - \dfrac{\alpha_{0dew}}{\alpha_0'})\ (\dfrac{\sin\phi_{su} - \sin\phi_{su*}}{1 - \sin\phi_{su*}})]$ $\quad (\mathrm{sunr.} \leq \mathrm{time} \leq \mathrm{time}(\phi_{su*}))$

3b. $m = 1.0$ $\quad (\mathrm{time} > \mathrm{time}(\phi_{su*}))$

4a. $\alpha_0 = \alpha_0'\ m\ c^{\sin\phi_{su}}$

5. FROM METHODOLOGY TO OPERATIONAL APPLICATIONS

5.1. Discussion of calculation results

The theory as developed for so far, have to be tested against all on site observations. First the measured reflectances were compared towards the $\alpha_0 = f(\alpha_0', \phi su, \overline{R_{swdf}}/\overline{R_{sw}})$ configuration. This was very usefull to determine the time required for dew evaporation, because variances between observed and fitted reflectances were quite clear during the dew evaporation process. Later on, the regression $\alpha_0 = f(\alpha_0', \phi su, \overline{R_{swdf}}/\overline{R_{sw}}, \theta)$ has verified to calculate proper early morning reflectance figures. Two examples are shown here; the sand-crust at Qaneitra, recorded on 11 November 1987 and the grey puffy at Qara, recorded on 5 November 1987.

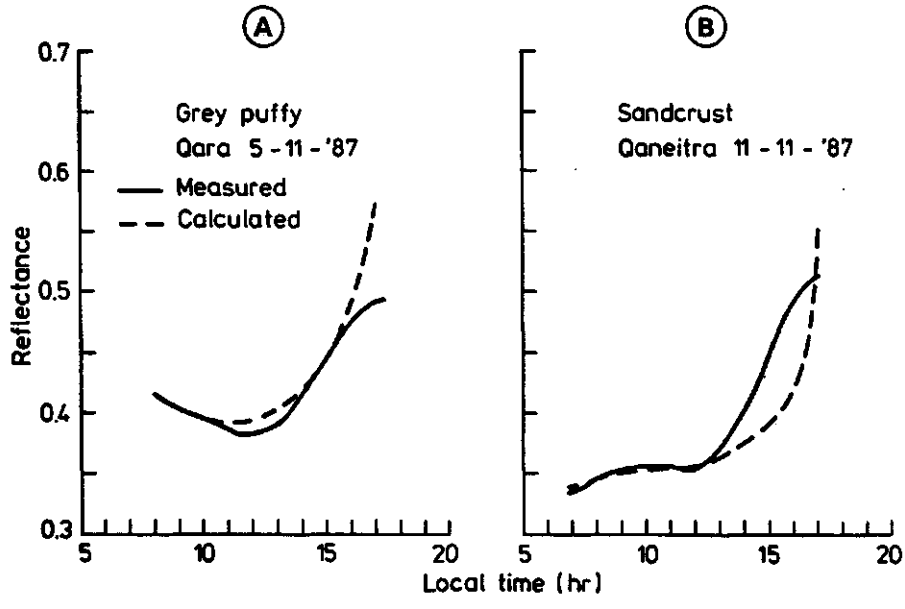

Fig. 6. Measured and calculated reflectances for 2 example spots
Grey puffy: $\alpha_0' = 0.170$, $\bar{c} = 2.682$, $\alpha_{0dew}/\alpha_0' = 0.85$
Sandcrust : $\alpha_0' = 0.124$, $\bar{c} = 4.148$, $\alpha_{0dew}/\alpha_0' = 0.65$

It may be concluded that the effect of dew can be conveniently described when the ratio α_{0dew}/α_0' is accurately known. Lower correlation is scored after 3 p.m. This has to do with comprehensive scattering features at low solar altitudes. When ϕ_{su} exceeds 65°, the irradiance flux becomes more uniform in all directions. The actual percentage of diffuse radiance will deviate much from the mean $\overline{R_{swdf}}/\overline{R_{sw}}$ ratio.

According eq. (13), this leads to a lower c coefficient with a consequently lower α_0 value, which is in good agreement with the former statements of MAKAROVA. An example will correct the situation of Fig. 4 and illustrate the benefit of the equation described in group 1c:

input: - time : 4.00 p.m.
- α_0(meas.) : 0.421
- α_0(cal.) : 0.492
- α_0' : 0.124
- $\overline{R_{swdf}/R_{sw}}$: 0.13
- R_{swdf}/R_{sw} : 0.20
- ϕ_{su} : 75.5 0

output: - $\bar{c}$ (group 1b) : 4.148
- c (group 1c) : 3.518
- α_0 (group 4a) : 0.419

The verification showed that the calculated results resemble the measured data very good. Hence, the method with a fixed α_0' value, based on $\bar{c}$ and a time dependant c value (group 1c) seems to be a correct estimation of the real reflectance. The serious problem here is that diurnal observations of R_{swdf}/R_{sw} are exceptionally recorded. This ratio can also be established by an experimental type of rotating band spectro-radiometer as developed by Guzzi. In a later stage of the project, diurnal spectral scattering and absorption effects will be assessed by this instrument and related with the $\bar{c}$ and c coefficients.

5.2. Definition of reference surface reflectances

Derived surface reflectances are only mutually comparable, if the view angle, moisture conditions and the diffuse support on the shortwave radiation budget are equal. This implies that all $\alpha_0'(\bar{c})$ values have to be transformed into standard $\alpha_0''(\bar{c}^*)$ values. A reference of $\bar{c}^*$ being 1.6 has been selected, because Bartman's formula accounts on a "mean atmosphere" which appears very close related with an optical depth of 0.60. This allows for comparible reflectances, at least for α'_0as described by Bartqan's formula and $\alpha_0''(c^*)$ only (see Fig. 7). The deviations appear to be rather small.

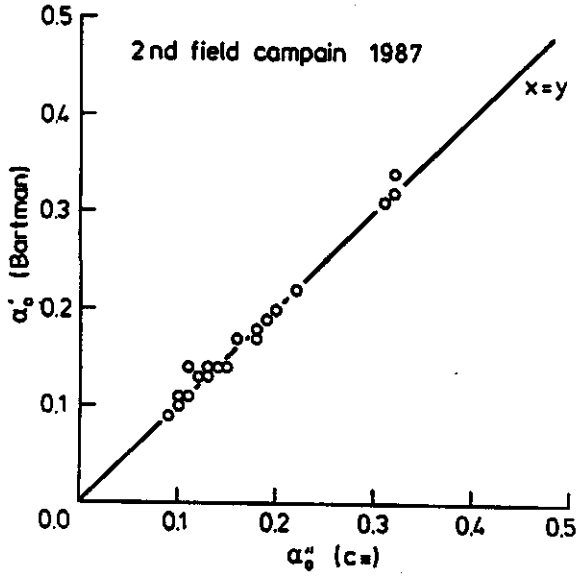

Fig. 7. Reference surface reflectances

5.3. Surface reflectance of arid regions

When agreement regarding reference conditions i.e. $\phi_{su} = 0$, $\bar{c}^* = 1.6$ (or $\tau = 0.6$, $\overline{R_{swdf}}/\overline{R_{sw}} = 0.4$) and $m = 1.0$ is reached, the reflectance ($\alpha''_0(\bar{c}^*)$) of all surfaces can be evaluated according table 10.

Table 10. Surface reflection coefficients for arid regions

Surface	Date	Site	$\bar{c}$	$\alpha'_0(\bar{c})$	$\alpha''_0(\bar{c}^*)$
White salt crust	15/3/87	E Siwa oasis	1.733	0.288	0.305
White salt crust	16/3/87	E Siwa oasis	1.192	0.387	0.314
White salt crust	5/11/87	NE Qara oasis	3.446	0.185	0.319
White salt crust	6/11/87	NE Qara oasis	1.044	0.479	0.354
White salt crust	14/2/78	NE Idri	1.219	0.487	0.402
White salt crust	15/2/78	NE Idri	1.660	0.415	0.426
White salt crust	2/9/78	NE Idri	1.523	0.333	0.322
White salt crust	4/9/78	NE Idri	1.356	0.351	0.312
Extremely dry soil	2/9/78	W Idri	1.331	0.396	0.348
Extremely dry soil	4/9/78	W Idri	1.144	0.380	0.300
Extremely dry soil	6/9/78	W Idri	1.222	0.340	0.281
Extremely dry soil	8/9/78	W Idri	1.160	0.349	0.278
Bare coarse sand	27/2/87	Bir Tarfawi	1.743	0.287	0.305
Bare coarse sand	27/2/87	Bir Tarfawi	1.786	0.281	0.304
Bare coarse sand	6/3/87	Bir Sharib	1.433	0.314	0.291
Bare coarse sand	10/3/87	SE Siwa oasis	1.101	0.412	0.316
Sandcrust on pediment	5/11/87	NE Qara oasis	2.724	0.181	0.264
Sandcrust on pediment	6/11/87	NE Qara oasis	1.339	0.310	0.273
Limestone	12/11/87	Qaneitra muh.	13.52	0.057	0.260
Sandcrust	6/3/87	Bir Sharib	1.365	0.265	0.237

Surface	Date	Site	$\bar{c}$	$\alpha_0'(\bar{c})$	$\alpha_0''(\bar{c}^*)$
Sandcrust	6/3/87	Bir Sharib	0.913	0.360	0.242
Sandcrust	11/11/87	Qaneitra muh.	1.970	0.211	0.245
Sandcrust	12/11/87	Qaneitra muh.	2.033	0.205	0.243
Sandcrust	6/3/87	Bir Sharib	1.127	0.296	0.231
Grey puffy	5/11/87	NE Qara oasis	2.436	0.182	0.245
Grey puffy	6/11/87	NE Qara oasis	1.039	0.366	0.270
Puffy with salt crust	11/3/87	W Siwa oasis	1.855	0.196	0.218
Puffy with salt cristals	11/3/87	W Siwa oasis	1.497	0.208	0.199
Grey brown puffy	11/11/87	Qaneitra muh.	2.291	0.133	0.171
Grey brown puffy	11/11/87	Qaneitra muh.	1.918	0.156	0.176
Grey brown puffy	12/11/87	Qaneitra muh.	3.080	0.103	0.164
Grey brown puffy	12/11/87	Qaneitra muh.	2.646	0.119	0.170
Grey brown puffy	11/3/87	W Siwa oasis	2.026	0.148	0.175
Grey brown puffy	11/3/87	W Siwa oasis	1.764	0.152	0.163
Open water sebkha	9/2/78	NNW Idri	5.628	0.069	0.169
Open water sebkha	9/2/78	NNW Idri	3.300	0.106	0.177
Dark grey puffy	10/3/87	SE Siwa oasis	1.180	0.157	0.127
Dark grey puffy	10/3/87	SE Siwa oasis	1.394	0.116	0.105
Dark grey puffy	10/3/87	SE Siwa oasis	1.232	0.149	0.124
Dark grey puffy	15/3/87	E Siwa oasis	1.907	0.095	0.108
Dark grey puffy	16/3/87	E Siwa oasis	1.001	0.139	0.100
Brown puffy	15/3/87	E Siwa oasis	1.734	0.127	0.135
Brown puffy	16/3/87	E Siwa oasis	0.798	0.206	0.126
Brown puffy	11/3/87	W Siwa oasis	2.469	0.097	0.132
Brown puffy	8/11/87	Quattara dep.	5.054	0.054	0.122
Brown puffy	8/11/87	Quattara dep.	3.469	0.080	0.139
Brown puffy	8/11/87	Quattara dep.	3.661	0.082	0.148
Dark grey puffy very wet	10/3/87	SE Siwa oasis	1.508	0.092	0.088
Wet sebkha	9/2/78	W Idri	2.569	0.162	0.227
Wet sebkha	11/2/78	W Idri	1.657	0.208	0.213
Wet sebkha	14/2/78	W Idri	1.413	0.202	0.185
Wet sebkha	15/2/78	W Idri	2.530	0.147	0.204
Wet sebkha	21/2/78	W Idri	3.397	0.118	0.202
Wet sebkha	22/2/78	W Idri	3.206	0.125	0.205
Hummocky with polygons	15/3/87	E Siwa oasis	1.536	0.191	0.186
Hummocky with polygons	16/3/87	E Siwa oasis	0.884	0.266	0.175
Brown hummocky	5/11/87	NE Qara oasis	2.639	0.124	0.177
Brown hummocky	6/11/87	NE Qara oasis	1.099	0.254	0.195
Brown hummocky	15/3/87	E Siwa oasis	1.533	0.149	0.145
Brown hummocky	16/3/87	E Siwa oasis	0.852	0.220	0.141
Sandy soft clay	8/11/87	Quattara dep.	4.013	0.068	0.129
Irrigated palms	21/2/78	Idri	3.528	0.123	0.216
Irrigated palms	22/2/78	Idri	4.442	0.107	0.221
Palms on dunes	6/9/78	Idri	2.054	0.184	0.220
Palms on dunes	8/9/78	Idri	2.121	0.182	0.222
Dusty acacia (20 cm)	27/2/87	Bir tarfawi	13.76	0.035	0.161
Green acacia (40 cm)	27/2/87	Bir Tarfawi	2.286	0.131	0.169
Dead acacia (10 cm)	27/2/87	Bir Tarfawi	1.763	0.173	0.185

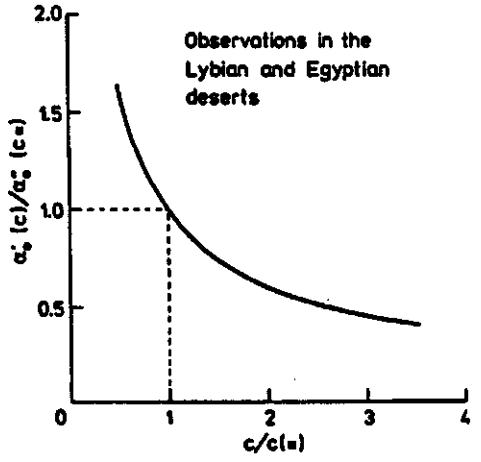

Fig. 8. Atmospherical effects on surface reflectance

On basis of the below presented $\alpha_0''(\bar{c}^*)$ figures and atmospherical information, a map with surface classification can be made from satellite images, applying the new reflectance equation (see table 11). It is even possible to estimate the surface wetness or the abundance of precipitated salts when the surface class (e.g. puffy) is known.

Table 11. Classified surface reflection coefficients for arid regions

Group	Surface	Mean $\alpha_0''(\bar{c}^*)$	standard deviation	number of replications
1	White salt crust	0.344	0.043	8
2	Extremely dry soils	0.302	0.028	4
3	Bare coarse sand	0.304	0.009	4
4	Sandcrust on pediment	0.269	0.004	2
5	Limestone	0.260	-	1
6	Sandcrust	0.240	0.002	5
7	Grey puffy	0.258	0.013	2
8	Puffy with salt crust	0.218	-	1
9	Puffy with salt cristals	0.199	-	1
10	Grey brown puffy	0.171	0.005	8
11	Dark grey puffy	0.113	0.011	5
12	Brown puffy	0.134	0.007	6
13	Very wet puffy	0.088	-	1
14	Wet sebkha	0.206	0.014	6
15	Hummocky with polygons	0.181	0.006	2
16	Brown hummocky	0.165	0.022	4
17	Sandy soft clay	0.129	-	1
18	Palms	0.220	0.002	4
19	Acacia	0.172	0.010	3

6. SUMMARY AND CONCLUSIONS

Surface reflectance is mostly considered as being constant (literature). However, environmental processes will effect the reflectance behaviour of natural materials considerably. Several authors suggested equations describing the diurnal variation of surface reflectance. Shortcoming of all these expressions is the incompleteness and the possibility to derive empirical coefficients of their equations. A new empirical equation accounting on solar altitude (ϕ_{su}), ratio of diffuse irradiance on the total irradiance budget ($\bar{c}$) and soil water content (m) is therefore proposed. The hypothesis was based on fieldwork done in the Western desert of Egypt. The developed theories were verified against measurements in the Lybian desert. On site observations in humid climates have not been performed sothat the functions dealing with atmosperical conditions can only be applied in a predefined range i.e. $\overline{R_{swdf}}/\overline{R_{sw}} = 0.12 - 0.44$.

Scattering of radiant energy by clouds, dust and aerosols can be conveniently described by the ratio $\overline{R_{swdf}}/\overline{R_{sw}}$. Diurnal variation of this ratio is, specially in subtropical countries, not always available. The evaluation of this diurnal variation will get more attention in a later project stage, when optical results of an experimental spectroradiometer will become available. When no figures of R_{swdf}/R_{sw} or $\overline{R_{swdf}}/\overline{R_{sw}}$ are known, a solution can be found to relate radiant energy patterns with the optical depth of Earth's atmosphere. The $\bar{c} = \bar{c}(\tau)$ relationship as calculated for Egypt confirms the $\bar{c} = \bar{c}(\tau)$ relationship of previous investigations in the Lybian Desert (1978). The correlation coefficient between $\bar{c}$ and τ is however with $r = 0.72$ not realy satisfactory.

The soil water content at surfacelevel is non-linear in respect to time and for this reason described by a sinusoidal function, using the ratio α_{0dew}/α'_0 as calculated by inversion of the new basic equation. Assumed hereby is a linear dependancy of reflectance on water content. By this way, no figures of on site surface water content have to be known, which is an important practical improvement.

The calculated and measured surface reflectance are nearly equivalent. Small differences are only found during the late afternoon. This has to do with the feature that the support of diffuse radiation becomes very high and deviate much from the mean $\overline{R_{swdf}}/\overline{R_{sw}}$ ratio. It is recommendable to work with c instead of $\bar{c}$ if values of R_{swdf}/R_{sw} are available in small time steps.

It must be emphasized that a reference surface reflectance have to be defined. Selected is $\alpha_0''(\bar{c}^*)$ i.e. $\phi_{su} = 0$, $c^* = 1.6$ and $m = 1.0$, because α_0' values as calculated by Bartman's formula were close related with $\alpha_0''(c^*)$. Transformation of observed reflectances as recorded at variable atmospherical conditions (time, location) into the referene reflectance shows promosing results. These compatible reference reflectances were for each type of surface in the same order of magnitude. This confirms the suggested theory. When a classification of the reflectances is made, the deviation between the mean classified reflectance and the reflectance of specific surface can be even an indication of the soil physical condition of that crust.

REFERENCES

BARTMAN, F.L. (1980). A time variable model of Earth's albedo, NASA CR-159259, United States. 123 p.

BERGH VAN DEN, B.P.J. and B.A.M. BOUMAN (1986) Theoretic reflection modelling of soil properties, proceedings of a symposium on Remote Sensing for Resources Developement and Environmental Management, Enschede, The Netherlands. p 331-334.

BUIJS, A. (1980) Statistiek om mee te werken (in Dutch), Leiden, The Netherlands. 248 p.

CARLSON, T.N. and P. WENDLING (1977) Reflected radiance measured by NOAA 3 VHRR as a function of optical depth for Saharian dust. Journal of Applied Meteorology 16. p 1368-1371.

KOEPKE, P. et al. (1985) The effect of surface reflection function and of atmospheric parameters on the shortwave radiation budget, Adv. Space Res. Vol. 5, No. 6, United Kingdom. p 351-354.

LARSON, J.C. and B.R. BARKSTROM (1977). Effects of realistic angular reflection laws for the Earth's surface upon calculations of the Earth - atmosphere albedo. Proceedings of a symposium on radiation in the atmosphere. p 451-453.

LIST R.J. (1968) Smithsonian Meteorological Tables, Smithsonian Institute, Washington, United States. 527 p.

MAKAROVA, N.M. et al.(1973). Generalized dependance of land and sea surfaces, albedos on sun elevation (in Russian). Trudy IPG 17. 210 p.

MENENTI, M. (1984). Physical aspects and determinations of evaporation in deserts applying remote sensing techniques, Report 10 (special issue), Wageningen, The Netherlands. 202 p.

——— (1986). An application of Thematic Mapper in Tunesia, ITC Journal 1986-1, Enschede, The Netherlands. p 35-42.

MONTEITH, J.L. (1973). Principles of environmental physics, Contemporary biology series, United Kingdom. 241 p.

MULDER, M.A. (1987). Remote sensing in soil science, Department of soil science and geology, Agricultural University of Wageningen, The Netherlands. 377 p.

ROSS, J. (1975) Radiative transfer in Plant Communities. In: J.L. Monteith, Vegetation and the Atmosphere, volume 1: Principles. Academic press. London. United Kingdom. p 13-55.

APPENDIX 1. Smithsonian Meteorological Table 132

TOTAL DAILY SOLAR RADIATION AT THE TOP OF THE ATMOSPHERE

(Explanation on p. 417.)

The solar constant J_e is assumed to be 1.94 cal. cm.$^{-2}$ min.$^{-1}$ Values apply to a horizontal surface.

	Longitude of the sun															
	0°	22½°	45°	67½°	90°	112½°	135°	157½°	180°	202½°	225°	247½°	270°	292½°	315°	337½°
	Approximate date															
	Mar. 21	Apr. 13	May 6	May 29	June 22	July 15	Aug. 8	Aug. 31	Sept. 23	Oct. 16	Nov. 8	Nov. 30	Dec. 22	Jan. 13	Feb. 4	Feb. 26
Latitude	cal. cm.$^{-2}$															
90°		423	772	999	1077	994	765	418								
80	155	423	760	984	1060	980	754	418	153	7						7
70	307	525	749	939	1012	934	742	519	303	129	24				24	131
60	447	635	809	934	979	929	801	629	442	273	146	72	49	73	146	276
50	575	732	867	958	989	954	859	725	568	414	286	204	176	205	289	419
40	686	807	910	972	991	967	901	798	677	545	429	348	317	350	434	553
30	775	865	929	967	975	960	921	856	765	663	564	492	466	494	568	670
20	841	894	923	935	935	930	916	884	831	760	685	627	605	630	691	769
10	882	897	893	881	873	877	886	887	871	835	789	748	733	752	795	845
0	895	873	837	804	790	800	830	863	885	886	870	851	843	855	878	896
−10	882	824	760	707	687	704	753	814	871	910	927	931	933	936	936	921
−20	841	750	660	593	567	590	654	741	831	907	959	988	999	993	968	918
−30	775	654	543	465	436	463	538	646	765	877	964	1020	1041	1025	973	888
−40	686	538	413	329	297	328	409	533	677	819	944	1027	1059	1032	953	828
−50	575	408	276	193	165	192	274	404	568	743	901	1014	1056	1018	909	752
−60	447	269	140	68	47	68	139	266	442	644	840	987	1046	992	847	652
−70	307	127	23				23	126	303	532	778	993	1081	998	785	539
−80	155	7						7	153	429	790	1041	1132	1046	796	434
−90										429	801	1056	1149	1062	809	434